The International Journal of Cardiovascular Imaging (2021) 37:135–144
https://doi.org/10.1007/s10554-020-01968-5

ORIGINAL PAPER

Evaluation of biventricular function in patients with COVID-19 using speckle tracking echocardiography

Omer Faruk Baycan[1] · Hasan Ali Barman[2] · Adem Atici[1] · Adem Tatlisu[1] · Furkan Bolen[1] · Pınar Ergen[1] · Sacit Icten[1] · Baris Gungor[3] · Mustafa Caliskan[1]

Received: 20 June 2020 / Accepted: 8 August 2020 / Published online: 15 August 2020
© Springer Nature B.V. 2020

Abstract

A new infectious outbreak sustained by severe acute respiratory syndrome coronavirus 2 (SARS-CoV-2) is now spreading all around the world. The aim of this study was to evaluate the prognostic value of left ventricular global longitudinal strain (LV-GLS) and right ventricular longitudinal strain (RV-LS) in patients with coronavirus disease 2019 (COVID-19). In this prospective, single-center study, data were gathered from patients treated for COVID-19 between April 15 and April 30, 2020. Two-dimensional echocardiography (2-DE) and speckle tracking echocardiography (STE) images were obtained for all patients. Patients were divided into three groups: those with severe COVID-19 infection, those with non-severe COVID-19 infection, and those without COVID-19 infection (the control group). Data regarding clinical characteristics and laboratory findings were obtained from electronic medical records. The primary endpoint was in-hospital mortality. A total of 100 patients hospitalized for COVID-19 were included in this study. The mean age of the severe group (n = 44) was 59.1 ± 12.9, 40% of whom were male. The mean age of the non-severe group (n = 56) was 53.7 ± 15.1, 58% of whom were male. Of these patients, 22 died in the hospital. In patients in the severe group, LV-GLS and RV-LS were decreased compared to patients in the non-severe and control groups (LV-GLS: − 14.5 ± 1.8 vs. − 16.7 ± 1.3 vs. − 19.4 ± 1.6, respectively [p < 0.001]; RV-LS: − 17.2 ± 2.3 vs. − 20.5 ± 3.2 vs. − 27.3 ± 3.1, respectively [p < 0.001]). The presence of cardiac injury, D-dimer, arterial oxygen saturation (SaO2), LV-GLS (OR 1.63, 95% confidence interval [CI] 1.08–2.47; p = 0.010) and RV-LS (OR 1.55, 95% CI 1.07–2.25; p = 0.019) were identified as independent predictors of mortality via multivariate analysis. LV-GLS and RV-LS are independent predictors of in-hospital mortality in patients with COVID-19.

Keywords Biventricular function · COVID-19 · Speckle tracking echocardiography

Introduction

Severe acute respiratory syndrome coronavirus 2 (SARS-CoV-2) is a novel RNA beta coronavirus, which causes the acute respiratory disease coronavirus disease 2019 (COVID-19) [1]. Although COVID-19 leads to multiple organ dysfunction or failure that affects the hepatic, renal, neurological systems, the involvement of the cardiovascular and respiratory systems are the most important predictors of morbidity and mortality [2]. Therefore, the early evaluation of whether these two systems are affected is crucial.

Many available studies have demonstrated that COVID-19 causes myocardial injury and left ventricular (LV) dysfunction. Myocardial injury has been found to be primarily associated with mortality and has been detected using troponin levels [3, 4]. There is not sufficient evidence to evaluate myocardial damage more specifically. In any case, severe lung disease can increase the right ventricular (RV) afterload, which may lead to impaired RV functions. Therefore, the evaluation of RV functions can provide information regarding the severity of the current COVID-19 [5]. Cardiac structure and functions are mainly evaluated by echocardiography. However, two-dimensional speckle tracking

✉ Hasan Ali Barman
drhasanali@hotmail.com

[1] Department of Cardiology, Faculty of Medicine, Goztepe Training and Research Hospital, Istanbul Medeniyet University, Istanbul, Turkey

[2] Department of Cardiology, Institute of Cardiology, Istanbul University – Cerrahpasa, Istanbul, Turkey

[3] Department of Cardiology, Dr. Siyami Ersek Training and Research Hospital, University of Health Sciences, Istanbul, Turkey

echocardiography (2D-STE) evaluates myocardial dysfunction and the subclinical impairment of myocardium earlier and more accurately than conventional echocardiography [6, 7]. LV global longitudinal strain (LV-GLS) has been demonstrated to estimate global LV myocardial tissue damage [8–10]. Additionally, RV longitudinal strain (RV-LS) viewed with 2D-STE has been shown to have a prognostic value [11]. In the present study, we evaluate whether any cardiac functions are affected when RV-LS and LV-GLS are found in COVID-19 patients with preserved RV and LV ejection fraction, which will provide important data regarding the prognosis and severity of COVID-19 and its cardiac effects.

The aim of this study is to evaluate the prognostic value of LV-GLS and RV-LS as they relate to in-hospital mortality and the correlation between the two in patients with COVID-19.

Methods

Study population

A total of 100 hospitalized patients with COVID-19 with normal LV ejection fraction (≥ 50%) between April 15 and April 30, 2020 were enrolled in this study. A total of 45 individuals who were age- and gender-matched normative population and had no history of cardiac disease were included as the control group. According to the World Health Organization interim guidance, the diagnosis of COVID-19 must be based on real-time reverse-transcription polymerase chain reaction (RT-PCR). As such, SARS-CoV-2 RNA was detected by a real-time RT-PCR method at the Public Health Microbiology Reference Laboratory of the Ministry of Health. Two-dimensional echocardiography (2DE) images were obtained for all patients. According to the severity of the COVID-19 infection, the patients were divided into two groups: severe and non-severe. Patients younger than 18 years of age, reduced LV ejection fraction (< 50%), the presence of segmental wall-motion abnormalities of the LV, severe valvular heart disease, coronary artery disease (CAD), atrial fibrillation, pulmonary hypertension (PHT), previous or current pulmonary embolism, severe chronic obstructive pulmonary disease, malignancy, or renal failure (< 30 ml/min) were excluded from the study. This study was approved by the institutional review board and the Republic of Turkey Ministry of Health.

Detailed data regarding patient demographics, clinical characteristics, medications, and laboratory findings were retrospectively collected from medical records. Upon being admitted to the hospital, the performed tests included a complete blood cell analysis and test to determine blood biochemistry, kidney function, electrolytes, C-reactive protein (CRP), high-sensitive troponin I (hs-TnI), and D-dimer. Computed tomography (CT) was used to confirm pneumonia. The primary endpoint was in-hospital mortality due to COVID-19.

Transthoracic 2DE and STE

Standard 2DE evaluation was performed in all patients using the X5 transducer (Philips Epiq7; Philips Healthcare, Inc., Andover, MA, USA) echocardiography device, and all measurements were conducted on the first day of admission by two experienced cardiologists who were blinded to the study design and patients' clinical data. Conventional echocardiographic measurements were performed according to the American Society of Echocardiography guidelines [12]. Echocardiographic images were obtained in the parasternal long-axis, short-axis, apical two-chamber, apical three-chamber, and apical four-chamber views with standard transducer positions. LV end-diastole diameter (LVEDD) and end-systole diameter (LVESD) and interventricular septal and posterior wall thicknesses were expressed in millimeters with M-mode echocardiography. LV ejection fraction (LVEF) was calculated using the modified Simpson's biplane method [13]. The left atrial (LA) diameter was measured from the parasternal long-axis view at end-systole, and the RV diameter was measured from the apical four-chamber view at the tricuspid annulus [14]. Pulsed wave Doppler velocity recordings were performed in the apical four-chamber views by placing the sample at the ends of the volume mitral valve. Mitral early peak velocity (E) and mitral late peak velocity (A) were recorded, and the E/A ratio was calculated. LV end-diastolic volume (LV EDV, ml) and end-systolic volume (LV ESV, ml) were calculated and stroke volume (EDV—ESV, ml) and cardiac output (stroke volume x heart rate, l/m) derived. Tricuspid annulus plane systolic excursion was conducted by the M-Mode, which was placed across the lateral tricuspid valve annulus on a four-chamber view. Systolic pulmonary artery pressure (sPAP) was measured by tricuspid regurgitation peak velocity. 2DE RV fractional area change was calculated on a four-chamber view by tracing the end-diastolic and end-systolic cavity and calculating the percentage change in area. The LV mass was calculated using the Devereux formula [15]. All measurements were corrected according to the body mass index (BMI).

Myocardial function was evaluated by 2D-STE with a quantitative analysis function of myocardial deformation. The end of diastole was defined as the peak R wave of the electrocardiogram, while the end of systole was defined as the time at which the aortic valve closed. Endocardial borders were monitored within the frame of 2D images at the end of systole. The epicardial border was determined by adjusting a wide myocardial width. The midpoints between the endocardial and epicardial borders and the middle

myocardial border were determined automatically. If necessary, manual adjustments were made to ensure correct tracking and to involve all LV wall thickness for 2D speckle viewing width. The analysis of LV-GLS was performed from the apical four-, three-, and two- chamber images. In the analysis, the QLAB-CMQ software program Philips Epiq 7C was used. Peak systolic strain measurements of each segment were automatically taken by a software (analysis) program. Longitudinal strain values of a total of 18 segments were obtained, and the mean value was determined as the global strain [16]. The analysis of RV-LS was performed from the apical four-chamber view. After tracing the RV endocardial border, the region of interest was automatically generated, and manual corrections were subsequently performed to fit the thickness of the RV myocardial wall. The RV free wall was automatically divided into three segments: basal, mid, and apical. RV-LS was calculated as the mean of the strain values of the three segments of the RV free wall. Segments that could not be tracked after manual adjustment by the operator were excluded.

The wall motion of each LV segment was visually evaluated on the basis of motion and systolic thickening in a 16-segment model (three segments per wall). Each segment was classified according to a conventional four-point scale (1, normokinesis; 2, hypokinesis; 3 akinesis; 4; dyskinesia). The wall motion score index (WMSI) was calculated by obtaining the average value of all segments of each location [14].

Definitions

The severe group consisted of patients with any of the following: (i) respiratory distress (respiratory rate: ≥ 30 breaths per min), (ii) an oxygen saturation of ≤ 93% at rest, (iii) a ratio of the partial pressure of arterial oxygen to the fractional concentration of oxygen inspired air of ≤ 300 mmHg, or (iv) a critical complication (septic shock, multiple organ dysfunction/failure that required admission to an intensive care unit (ICU), and/or any type of respiratory failure that required mechanical ventilation) [17]. Patients with clinical symptoms who were hospitalized but did not meet severe criteria were included in the non-severe group. Acute cardiac injury was defined as hs-TnI serum levels above the 99th percentile upper reference limit [18].

Statistical analyses

All statistical tests were conducted using the Statistical Package for the Social Sciences 21.0 for Windows (SPSS Inc., Chicago, IL, USA). The Kolmogorov–Smirnov test was used to analyze the normality of the data. Continuous data are expressed as mean ± standard deviation (SD), and categorical data are expressed as percentages. A chi-square test was used to assess the differences in categorical variables between the groups. A Student's t-test or the Mann–Whitney U test was used to compare unpaired samples as needed. The relationships among the parameters were assessed using Pearson's or Spearman's correlation analysis according to the normality of the data. Primary analysis used ANOVA to compare all reported data for parametric variables, whereas the Kruskal–Wallis test was used for comparison among non-parametric variables between the severe subjects, non-severe subjects, and controls. Univariate and multivariate logistic regression analyses were used to identify the independent variables of mortality. After performing univariate analysis, the stepwise method was used to select significant obtained variables for use in the multivariate logistic regression analysis. The results of the univariate and multivariate regression analyses are presented as odds ratios with 95% confidence intervals (CIs). For the echocardiographic parameter of strain including LV-GLS and RV-LS, receiver operating characteristic (ROC) curves were obtained, and the optimal values with the greatest total sensitivity and specificity in the prediction of mortality were selected. Cumulative survival curves were derived according to the Kaplan–Meier method. Reproducibility was assessed by reanalyzing 20 randomly selected patients (reported as intra-observer reliability) and calculating from a second independent observer (reported as inter-observer reproducibility). Significance was assumed at a two-sided $p < 0.05$.

Results

Clinical characteristics

A total of 145 patients were included in the present study. Of these, 100 had tested positive for COVID-19; their clinical and demographic characteristics are shown in Table 1. There was no statistically significant difference between the groups in terms of gender, age, BMI, heart rate (HR), systolic arterial pressure, diastolic arterial pressure, or smoking. The number of respiratory rate (RR) was significantly higher in the severe group compared to the control and non-severe groups ($p < 0.001$). Similarly, lung involvement was detected in all patients of the severe group by CT imaging; 55% of the non-severe group demonstrated lung involvement, and the difference was statistically significant ($p < 0.001$). When the groups were compared in terms of the presence of chronic illness (hypertension [HTN], diabetes mellitus [DM], hyperlipidemia), there was no statistically significant difference among them. While there was no statistical difference between the laboratory findings in terms of white blood cell, creatinine, sodium, potassium, or creatine kinase-MB levels, the levels of glucose, CRP, hs-TnI and D-dimer were statistically significantly higher

Table 1 Demographic and clinical characteristics of patients severe and non-severe group

Variables	Total patients (n = 145)	Control (n = 45)	Non-severe (n = 56)	Severe (n = 44)	p
Clinical characteristics					
Age (years)	55.6 ± 14.4	54.6 ± 14.7	53.7 ± 15.1	59.1 ± 12.9	0.152
Male, n(%)	73 (50%)	22 (48%)	33 (58%)	18 (40%)	0.196
BMI (kg/m_2)	23.4 ± 3.4	23.7 ± 3.4	23.0 ± 2.9	23.5 ± 4.1	0.578
HR, beats/min	86.9 ± 18.0	83.6 ± 15.6	85.3 ± 16.0	92.2 ± 21.6	0.055
RR, times/min	23.3 ± 4.1	21.8 ± 2.3 [a]	21.3 ± 2.3 [e]	27.5 ± 4.4 [a e]	< 0.001
SAP, mmHg	123.0 ± 15.8	125.6 ± 13.6	121.1 ± 14.5	122.7 ± 19.3	0.363
DAP, mmHg	76.9 ± 8.3	77.0 ± 7.9	76.8 ± 8.3	77.0 ± 8.7	0.986
Smoker, n (%)	44 (30%)	13 (28%)	21 (37%)	10 (22%)	0.271
Pneumonia on CT, n (%)	75 (51%)	–	31 (55%)	44 (100%)	< 0.001
Chronic medical illness					
HT, n(%)	43 (29%)	11 (24%)	15 (26%)	17 (38%)	0.285
DM, n(%)	25 (17%)	7 (15%)	8 (14%)	10 (22%)	0.506
HLD, n(%)	20 (13%)	8 (17%)	5 (8%)	7 (15%)	0.390
Laboratory findings					
Haemoglobin(g/dl)	12.5 ± 2.0	12.9 ± 1.6[a]	13.2 ± 1.2 [e]	11.1 ± 2.6[a, e]	< 0.001
WBC (10^3 /μl)	6.6 (5.1–11.4)	6.1 (5.1–10.8)	6.1(5.1–10.8)	9.1(5.2–13.7)	0.251
Creatinine (mg/dl)	0.8 (0.7–1.0)	0.8 (0.7–1.0)	0.8 (0.7–1.0)	0.8 (0.7–1.2)	0.968
Sodium (mmol/L)	136.6 ± 3.3	136.9 ± 3.1	136.8 ± 2.8	135.9 ± 4.0	0.254
Potassium (mmol/L)	4.1 ± 0.5	4.0 ± 0.6	4.1 ± 0.5	4.0 ± 0.5	0.456
Glucose (mg/dL)	122.7 ± 30.4	114.4 ± 18.6[a]	116.4 ± 28.9 [e]	139.3 ± 35.7[a e]	< 0.001
CRP (mg/dL)	43 (15–81)	–	29 (9–61)	81 (46–132)	< 0.001
hs-TnI (NR < 14 pg/mL)	10 (10–17)	–	10 (10–11)	16 (10–59)	< 0.001
D-dimer (ng/mL)	690 (327–1020)	–	420 (192–690)	1140 (707–1700)	< 0.001
CK-MB (ng/mL)	5.0 (1.1–11.0)	–	5.2 (1.1–9.1)	5.0 (1.2–17.0)	0.756
SaO2	93.3 ± 4.7	96.3 ± 1.3[a]	95.7 ± 2.3[e]	87.3 ± 3.6[a e]	< 0.001
Treatments					
Antiviral therapy, n (%)	84 (58%)	–	48 (85%)	36 (81%)	0.598
Antibiotic therapy, n (%)	94 (65%)	–	52 (92%)	42 (95%)	0.587
Oxygen therapy, n (%)	20 (14%)	–	20 (35%)	0 (0%)	< 0.001
High-flow oxygen, n (%)	26 (18%)	–	0 (0%)	26 (59%)	< 0.001
NIMV, n (%)	20 (13%)	–	0 (0%)	20 (45%)	< 0.001
ICU admission, n (%)	33 (22%)	–	0 (0%)	33 (75%)	< 0.001
Complications					
Acute heart injury, n (%)	36 (24%)	–	5 (9%)	31 (70%)	< 0.001
Acute kidney injury, n (%)	31 (21%)	–	3 (5%)	28 (63%)	< 0.001
Prognosis					
Hospital stay (days)	9 (5–13)	–	6 (4–10)	13 (9–0)	< 0.001
Discharge, n (%)	60 (41%)	–	46 (82%)	14 (31%)	< 0.001
Death, n (%)	22 (15%)	–	0 (0%)	22 (50%)	< 0.001

BMI body mass index, *HR* heart rate, *RR* respiratory rate, *SAP* systolic arterial pressure, *DAP* diastolic arterial pressure, *HT* hypertension, *DM* diabetes mellitus, *HLD* hyperlipidemia, *WBC* white blood cell, *CRP* C-reactive protein, *hs-TnI* high sensitive-Troponin I, *NR* normal range, *CK* creatinine kinase, *SaO2* arterial oxygen saturation, *NIMV* non invasive mechanical ventilation, *ICU* intensive care unit

[*] $P < 0.05$ Between control group and non-severe group,

[a] $P < 0.05$ between control group and severe group

[e] $P < 0.05$ between non-severe group and severe group

than in the non-severe group. Likewise, hemoglobin (Hgb) and arterial oxygen saturation (SaO2) levels were also statistically significantly lower in the severe group compared to the non-severe and control groups. When the patients in the severe and non-severe groups were compared in terms of the treatment they received, there was no statistically significant difference between the groups in terms of antiviral and antibiotic treatment, while the oxygen therapy, high flow oxygen therapy, and non-invasive ventilation rates were statistically significantly higher in the severe group. Similarly, ICU admission, acute cardiac injury, and acute kidney injury rates were found to be statistically significantly higher in the severe group than in the non-severe group. Finally, discharge and mortality rates were compared between the severe and non-severe groups. The discharge rates were high in the non-severe group; no mortality was observed in this group. However, in the severe group, the discharge rate was low, and 22 deaths were observed. There was a statistically significant difference between the groups in terms of discharge and death. The median hospital stay was six days in the non-severe group and 13 days in the severe group, and there was a statistically significant difference between the two groups ($p < 0.001$) (Table 2).

Echocardiographic characteristics

Using 2D-STE, the conventional echocardiography parameters and GLS parameters of the three groups were compared. A comparison of the LVEF, stroke volume (SV), cardiac output (CO), LVEDD, LVESD, LV mass, WMSI, left atrium (LA), the E/A ratio, and the E/e' ratio of the three groups revealed no statistically significant difference. The LV-GLS values of the control, non-severe, and severe groups were $-19.4 \pm 1.6\%$, $-16.7 \pm 1.3\%$, and $-14.5 \pm 1.8\%$, respectively, and there was a statistically significant difference among the three groups ($p < 0.001$). It was observed that the sPAP value, which is one of the conventional parameters, was statistically significantly higher in the severe group compared to the other groups. In addition, the RV diameter was found to be higher in the severe group compared to the other groups, The RV-LS values of the control, non-severe, and severe groups were $-27.3 \pm 3.1\%$, $-20.5 \pm 3.2\%$, and $-17.2 \pm 2.3\%$,

Table 2 Comparison of conventional echocardiographic and two-dimensional speckle tracking global longitudinal strain parameters of patients

Variables	Total patients (n = 145)	Control(n = 45)	Non-severe (n = 56)	Severe (n = 44)	p
Left heart findings					
LVEF (%)	60.3 ± 4.6	60.8 ± 3.7	59.9 ± 4.9	58.1 ± 4.6	0.117
LV-GLS (%)	− 16.8 ± 2.5	− 19.4 ± 1.6* [a]	− 16.7 ± 1.3* [e]	− 14.5 ± 1.8[a e]	< 0.001
SV (mL)	66.7 ± 18.6	68.8 ± 11.8	65.6 ± 13.4	65.9 ± 28	0.660
CO(L/min)	5.9 ± 2.1	6.4 ± 1.7	5.6 ± 1.6	5.7 ± 2.7	0.101
LVEDD (mm)	46.2 ± 4.4	46.6 ± 4.4	46.2 ± 4.1	45.8 ± 4.9	0.669
LVESD (mm)	30.1 ± 3.9	29.9 ± 3.4	30 ± 3.5	30.6 ± 4.9	0.684
LV mass (g)	166.9 ± 19.8	165.7 ± 19.1	167.1 ± 18.8	168.1 ± 21.7	0.531
WMSI	1 ± 0.2	1 ± 0.2	1 ± 0.1	1 ± 0.2	0.614
LA (mm)	30.0 ± 4.6	33.3 ± 4.4 [a]	34.5 ± 3.3[e]	37.3 ± 5.4 [a e]	< 0.001
E/A ratio	1 ± 0.3	1 ± 0.4	1 ± 0.3	0.9 ± 0.3	0.551
E/e' ratio	9.2 ± 2.5	8.7 ± 2.7	9.1 ± 2.1	9.9 ± 2.9	0.114
Right heart findings					
RV-FAC (%)	45.2 ± 5.3	46.4 ± 5.4	45.1 ± 4.8	44.1 ± 5.6	0.127
RV-LS (%)	− 21.6 ± 5	− 27.3 ± 3.1* [a]	− 20.5 ± 3.2* [e]	− 17.2 ± 2.3 [a e]	< 0.001
TAPSE (mm)	21.8 ± 3.3	22.4 ± 3.3	22.1 ± 3.3	21 ± 3.3	0.146
sPAP, mmHg	31 ± 8.3	28.6 ± 5.3 [a]	28.7 ± 6.3 [e]	36.5 ± 10.4 [a e]	< 0.001
RV (mm)	31.8 ± 4.5	29.9 ± 2.8 [a]	31.7 ± 4.2	33.7 ± 5.6 [a]	< 0.001
RA (mm)	32.9 ± 4.4	31.7 ± 2.9	33.2 ± 4.5	33.9 ± 5.3	0.063
TDI S', cm/s	15.2 ± 3.1	15.5 ± 3.2	15 ± 3.1	15.1 ± 3	0.721
PA, mm	21.4 ± 2.6	20.9 ± 2.8	21.3 ± 2.6	22.1 ± 2.1	0.080

LVEF left ventricular ejection fraction, *LV-GLS* left ventricular global longitudinal strain, *SV* stroke volume, *CO* cardiac output, *LVEDD* left ventricular end diastolic diameter, *LVESV* left ventricular end systolic diameter, *WMSI* wall motion score index, *LA* left atrial, *RV-FAC* right ventricular fractional area change, *RV-LS* right ventricular longitudinal strain, *TAPSE* tricuspid annular plane systolic excursion, *sPAP* systolic pulmonary artery pressure, *RV* right ventricular, *RA* right atrial, *TDI S'* tissue Doppler imaging systolic wave S' velocity, *PA* pulmonary artery

[*] $P < 0.05$ Between control group and non-severe group

[a] $P < 0.05$ between control group and severe group

[e] $P < 0.05$ between non-severe group and severe group

respectively, indicating a statistically significant difference among the groups ($p < 0.001$) (Fig. 1).

The relationships of the LV-GLS and RV-LS values with age, hs-TnI, D-dimer, CRP, Hgb, sPAP, SaO2, RR, and HR were evaluated via Spearman's or Pearson's correlation analyses. A statistically significant relationship was detected between the LV-GLS value and hs-TnI, D-dimer, and sO2, as seen in Table 3.

Predictors of mortality

Of the patients in this study, 22 died in the hospital (Fig. 2). The parameters affecting mortality were evaluated by including LV-GLS and RV-LS in the two models separately using logistic regression analysis with univariate and multivariate analysis. Age, gender, HT, DM, CRP, cardiac injury, D-dimer, LV-GLS, RV-LS, RR, SaO2, and sPAP were first evaluated using univariate analysis. Age, gender, cardiac injury, D-dimer, SaO2, LV-GLS, and RV-LS, which were statistically significant in the univariate analysis, were then reevaluated in a multivariate analysis. In the first model of Table 4, cardiac injury (OR 5.125, $p = 0.027$), SaO2 (OR 0.842, $p = 0.025$), LV-GLS (OR 1.635, $p = 0.010$), and LV-GLS > − 15.20% (OR 8.342, $p < 0.001$) were thus determined to be independent predictors of mortality. The second model of Table 4 was

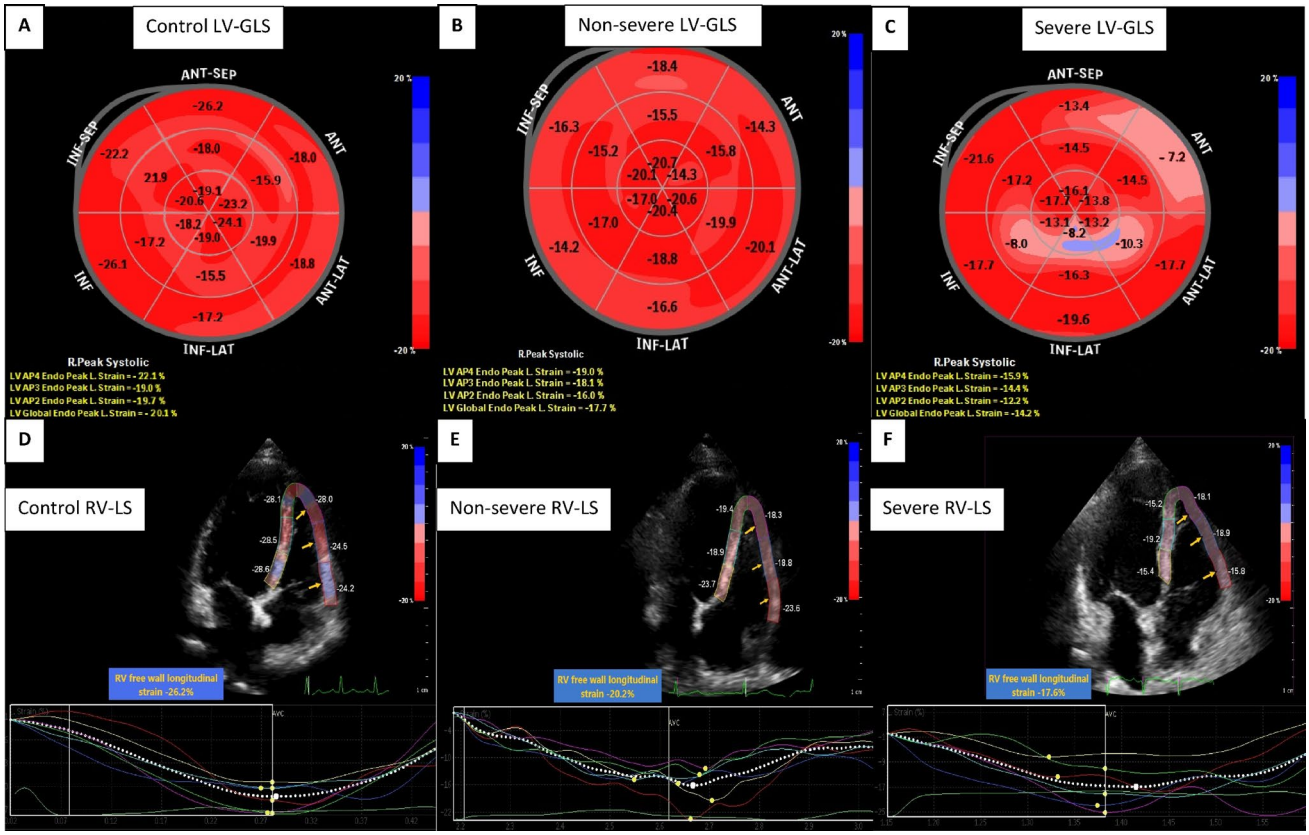

Fig. 1 Bull's eye images of right ventricular longitudinal strain (RV-LS) values of control, non severe and severe patients

Table 3 Correlation of strain findings with prognostic laboratory parameters

	Spearman	RV-LS	Age	hs-TnI	D-dimer	CRP	Hgb	sPAP	SaO2	RR	HR
LV-GLS	*r*	0.794	0.065	0.633	0.577	0.175	0.062	0.355	−0.549	0.396	0.206
	p	< 0.001	0.437	< 0.001	< 0.001	0.168	0.460	< 0.001	< 0.001	< 0.001	0.013
RV-LS	*r*		0.108	0.608	0.620	0.158	0.111	0.385	−0.608	0.492	0.123
	p		0.197	< 0.001	< 0.001	0.351	0.184	< 0.001	< 0.001	< 0.001	0.141

LV-GLS left ventricular global longitudinal strain, *RV-LS* right ventricular longitudinal strain, *hs-TnI* high-sensitive troponin I, *CRP* C-reactive protein, *Hgb* haemoglobin, *sPAP* systolic pulmonary artery pressure, *SaO2* arterial oxygen saturation, *RR* respiratory rate, *HR* heart rate

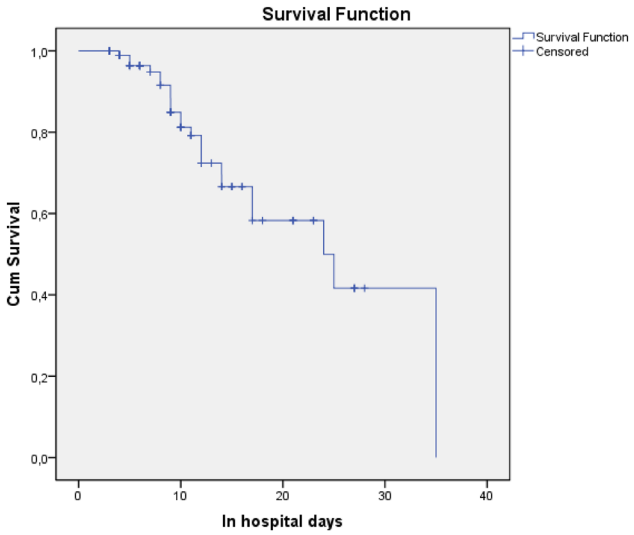

Fig. 2 Kaplan–Meier survival curves for mortality during the time from admission

created by removing the LV-GLS and adding the RV-LS to predict mortality development. In this second model, cardiac injury (OR 1.417, p = 0.031), D-dimer (OR 4.250, p = 0.021), SaO2 (OR 0.830, p = 0.012), RV-LS (OR 1.557, p = 0.019), and RV-LS > − 18.45% (OR 6.229, p = 0.011) were thus determined to be independent predictors of mortality (Table 4).

We evaluated the specificity and sensitivity of the LV-GLS and RV-LS values that were significant in the multivariate analysis with ROC analysis to predict mortality development in patients. The blue line represents LV-GLS, and the green line represents RV-LS; the area under the curve (AUC) of each was 0.83 (0.74–0.92) and 0.77 (0.66–0.88), respectively. The LV-GLS value predicts mortality development with 77% sensitivity and 75% specificity with a − 15.20 cutoff value, and the RV-LS value predicts mortality development with 72% sensitivity and 66% specificity with a − 18.45 cutoff value (Fig. 3).

Reproducibility

A total of 20 patients were randomly selected for intra- and interobserver variability analysis. The compatibility of intra- and interobserver LV-GLS, RV-LS, and WMSI values were calculated. The correlation coefficient for intra- and interobserver variability was evaluated, and the following results were obtained—intraobserver: 0.94 (95% CI, 0.91–0.96), interobserver: 0.90 (95% CI 0.84–0.95) for LV-GLS; intraobserver: 0.92 (95% CI 0.88–0.94), interobserver: 0.89 (95% CI 0.82–0.94) for RV-LS; intraobserver: 0.89 (95% CI 0.84–0.94), and interobserver:0.86 (95% CI 0.77–0.94) for WMSI.

Discussion

We evaluate the prognostic value of LV-GLS and RV-LS in patients with COVID-19. The principal findings of our study are as follows: (i) LV-GLS and RV-LS were lower in the severe group compared to the non-severe group; (ii) cardiac injury, D-dimer, SaO2, LV-GLS, and RV-LS were found to be independent predictors of mortality through multivariate analysis.

The structure and function of the LV are commonly assessed by echocardiography. STE quantifies myocardial deformation globally and regionally, regardless of the insonation angle or cardiac translational movements. It is an objective and reproducible method [19, 20]. Direct strain measurement from 2D grayscale images makes STE a better tool than 2DE for the evaluation of cardiac mechanics. Furthermore, STE is a more useful method for evaluating global and regional myocardial deformations compared to tissue Doppler imaging as it is accurate, highly reproducible, angle-independent, and does not require a fixed angle of insonation [21, 22].

Due to the fact that subendocardial cardiac fibers are particularly and primarily sensitive to the deleterious effects of fibrosis; diseases such as HTN, CAD, DM, and obesity may

Table 4 Multivariate Logistic Regression analysis on the risk factors associated with mortality in patients with COVID-19

Variable	OR	95% CI	P	Variable	OR	95% CI	P
Age	0.984	0.930–1.042	0.588	Age	0.986	0.928–1.046	0.637
Gender	2.942	0.723–11.970	0.132	Gender	3.049	0.721–12.899	0.130
Cardiac injury	5.125	1.206–21.783	0.027	Cardiac injury	1.417	1.125–1.709	0.031
D-dimer	1.001	0.999–1.003	0.792	D-dimer	4.250	1.312–21.418	0.021
SaO2	0.842	0.724–0.979	0.025	SaO2	0.830	0.717–0.961	0.012
LV-GLS	1.635	1.080–2.474	0.010	RV-GLS	1.557	1.075–2.256	0.019
*LV-GLS > —15.20%	8.342	2.779–79.351	< 0.001	*RV-GLS > − 18.45%	6.229	1.512–25.670	0.011

SaO2 arterial oxygen saturation, *LV-GLS* left ventricular global longitudinal strain, *RV-LS* right ventricular longitudinal strain

*LV-GLS and RV-GLS were analyzed in logistic regression separately as linear and categorical variables

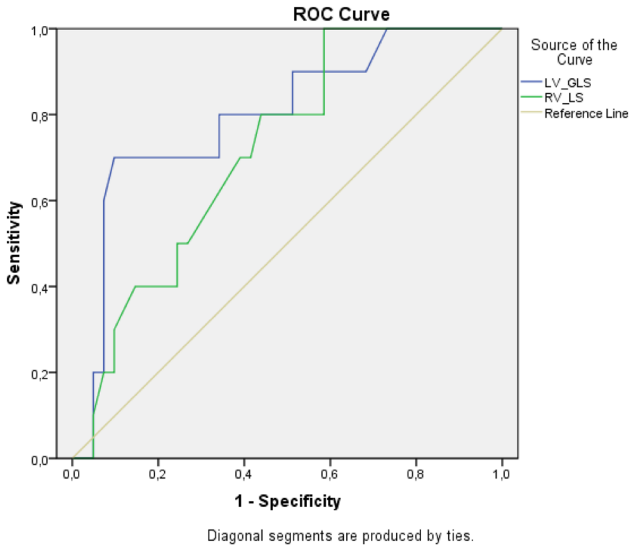

Fig. 3 ROC curve analysis showing the specificity and sensitivity of the LV-GLS and RV-LS in predicting death

induce fibrotic processes of the LV with preserved EF by affecting the subendocardial fibers which provide longitudinal systolic functions in the beginning [23, 24]. Shah et al. and Donal et al. designed multicentric studies and enrolled a large number of patients. These two studies have assessed the association of LV-GLS with poor cardiovascular outcomes in patients with heart failure with preserved EF [25, 26]. A meta-analysis including 794 patients with severe sepsis and/or septic shock showed that LV-GLS measurements were strongly associated with survival (standard mean difference, − 0.26; 95% CI − 0.47, − 0.04; p = 0.02), while LV ejection fraction was not found to be a predictor of mortality [27]. In our study, although there was no statistically significant difference among the three groups in terms of the conventional echocardiography parameters of LV, there was a statistically significant difference among the LV-GLS values of the patients in the three groups.

Zhaohai Zheng et al. analyzed 13 meta-analyses and examined 3027 patients with COVID-19; they found that elevated troponin and D-dimer levels were related to the severity of the disease and mortality. Elevated troponin levels are frequently present in patients with COVID-19 and are significantly associated with myocardial injury and fatal outcomes [28, 29]. As expected, increased troponin levels showing myocardial damage were also associated with the disruption in the LV-GLS, which is evidence of myocardial tissue impairment. In our study, there was a statistically significant relationship between the LV-GLS value, hs-TnI, and D-dimer levels. In a study of 61 unstable patients with angina, the LV-GLS value was found to be better in 48 patients who underwent invasive coronary angiography (ICA) and did not have significant coronary artery stenosis (− 19.4 vs. − 15.9%, p < 0.001). Patients who did not undergo ICA had a better LV-GLS value (− 20.2 vs. − 17.7%, p = 0.017) [30]. In our study, LV-GLS was also impaired in patients in the non-severe COVID-19 group with relatively low troponin levels. In patients with normal EF who have an underlying cardiac disease, LV-GLS might be impaired even if hs-TnI is negative. In a case report, it was determined that the RV was affected as well as the LV in the patient with COVID-19 [31]. Cardiac chambers with greater volumes are interdependent on prolonged exposure to higher pressures. When chamber pressures increase, cardiac troponin is released, and the increased wall strain may lead to subendocardial ischemia and injury [32, 33]. In our study, there was a statistically significant relationship between RV-LS values and both hs-TnI and D-dimer levels.

In a recent study by Li et al. involving 120 patients with COVID-19, RV-LS was identified as an independent predictor of mortality [34]. In this study, the best cutoff value of RV-LS for outcome prediction was − 23% (AUC, 0.87; P < 0.001; sensitivity, 94.4%; specificity, 64.7%). In this study, only RV-LS was evaluated, and no examination was conducted regarding how LV-GLS is affected by COVID-19 and its prognosis. In this study, patients with low ejection fraction were also included. In our study, the prognostic significance of LV-GLS in relation to RV-LS was investigated. Patients with a low ejection fraction were excluded, and the biventricular function was evaluated by STE in patients with COVID-19 with preserved ejection fraction. To our knowledge, no study has evaluated the prognostic value of the LV function with LV-GLS or the relationship between RV-LS and LV-GLS using 2D-STE in patients with COVID-19. We also found that a correlation between LV-GLS and RV-LS and that the values decrease as the severity of the COVID-19 infection increases.

In the recent times, studies showed the presence of myocardial dysfunction using echocardiography in intensive care patients diagnosed with sepsis who are receiving mechanical ventilation [35, 36]. In these studies, it was observed that almost 30–40% of sepsis patients developed a decrease in LVEF and diastolic dysfunction. Hyperdynamic heart functions because of systemic inflammatory response, increase of cardiac output (CO) and LVEF are observed in the early period in these sepsis patients. In the late period, extensive myocardial injury occurs due to severe hypoxia and inflammation [37]. Previous studies have shown right heart function impairment in patients with acute respiratory distress syndrome (ARDS) [38, 39]. The extent of RV dysfunction has been shown to be an important predictor of mortality in different patient groups. Right heart dysfunction come into prominence in determining circulation and respiratory management strategies, especially in patients with COVID-19 with lung involvement. Our results showed that patients with a more severe clinical state present more severe cardiac

dysfunction; but it is not clear whether this can be imputable to COVID-19 or this is a general outcome that can be expected in non-COVID-19 patients with similarly severe clinical conditions (respiratory disease).

There are several publications regarding the possible mechanisms of cardiac damage observed in patients with COVID-19 [1–4]. Myocardial injury detected with increased troponin levels was found to be related to both the severity of the disease and mortality. Moreover, patients with cardiovascular diseases appear to have a potentially fatal with different mechanisms including myocardial damage, cytokine storm, myocarditis, and microembolism. The related mechanisms are summarized as follows: (i) Cytokine storm and multiple organ failure due to acute systemic inflammatory response; (ii) an imbalance between the oxygen supply and demand of the myocardium secondary to severe hypoxia resulting from acute respiratory failure; (iii) cardiotoxicity that may develop due to the agents used in the treatment; (iv) coronary thrombosis caused by plaque rupture as a result of shear stress caused by increased coronary circulation with systemic inflammation; (v) a tendency to arrhythmia that occurs due to an electrolyte imbalance in the renin-angiotensin aldosterone system in relation to the ACE-2 signaling system of the virus; (vi) embolic complications caused by the tendency to thrombosis due to systemic inflammation; and vii) myocarditis possibly caused by the direct entry of the virus (although not yet proven for myocardium) into the cell by binding to the ACE-2 receptor, which is predominantly expressed in lung and heart tissue, and causing changes in the ACE2 signaling system. Considering this mechanisms, the myocardial tissue of a RV affected by the current respiratory condition may be affected in the early stages of the disease process, and RV-LS decreases in patients with COVID-19. One of the mechanisms of cardiac effects causing mortality in patients with COVID-19 has been identified as myocardial disruption at the tissue level. For this reason, LV and RV longitudinal strain are the main factors of prognosis due to COVID-19 early and more pronounced effect compared to other conventional echocardiography parameters.

Our study is limited in several ways. First, the data was derived from a single center, and the sample size was relatively small. Second, there was a lack of measurement of the strain on the left atrium. Third, no 2DE data was obtained from patients prior to COVID-19 infection. Fourth, echocardiography images were recorded by one person due to the risk of infection but evaluated by two physicians.

In conclusion, we have determined that both RV-LS and LV-GLS were affected by COVID-19 and are parameters of independent predictors of mortality in patients with COVID-19. RV dysfunction can be detected using echocardiography, which can provide early information regarding the severity of the COVID-19 infection, which may in turn help to guide the treatment of this group of patients.

Funding The author(s) received no financial support for the research, author- ship, and/or publication of this article.

Compliance with ethical standards

Conflict of interest All authors declare that they have no conflict of interest.

References

1. Li Q, Guan X, Wu P et al (2020) Early transmission dynamics in Wuhan, Chin, of novel coronavirus- ınfected pneumonia. New Engl J Med 382:1199
2. Guan W-J, Ni Z-Y, Hu Y, Liang W-H, Ou C-Q, He J-X et al (2020) Clinical characteristics of coronavirus disease 2019 in China. New Engl J Med. https://doi.org/10.1056/NEJMoa2002032
3. Shi S, Qin M, Shen B et al (2020) Association of cardiac injury with mortality in hospitalized patients with COVID-19 in Wuhan China. JAMA Cardiol 5:802
4. Lippi G, Lavie CJ, Sanchis-Gomar F (2020) Cardiac troponin I in patients with coronavirus disease 2019 (COVID-19): evidence from a meta-analysis. Prog Cardiovasc Dis. 63:390
5. Tello K, Gall H, Richter M et al (2019) Right ventricular function in pulmonary (arterial) hypertension. Herz 44(6):509–516
6. Carluccio E, Biagioli P, Alunni G et al (2018) Prognostic value of right ventricular dysfunction in heart failure with reduced ejection fraction: superiority of longitudinal strain over tricuspid annular plane systolic excursion. Circ Cardiovasc Imaging 11:e006894
7. Xie M, Li Y, Cheng TO et al (2015) The effect of right ventricular myocardial remodeling on ventricular function as assessed by two-dimensional speckle tracking echocardiography in patients with tetralogy of Fallot: a single center experience from China. Int J Cardiol 178:300
8. Nucifora G, Schuijf JD, Delgado V et al (2010) Incremental value of subclinical left ventricular systolic dysfunction for the identification of patients with obstructive coronary artery disease. Am Heart J 159:148–157
9. Leitman M, Lysyansky P, Sidenko S et al (2004) Two-dimensional strain- a novel software for real-time quantitative echocardiographic assessment of myocardial function. J Am Soc Echocardiogr 17:1021–1029
10. Adamo L, Perry A, Novak E, Makan M, Lindman BR, Mann DL (2017) Abnormal global longitudinal strain predicts future deterioration of left ventricular function in heart failure patients with a recovered left ventricular ejection fraction. Circ Heart Fail 10:e003788
11. Park SJ, Park JH, Lee HS et al (2015) Impaired RV global longitudinal strain is associated with poor long-term clinical outcomes in patients with acute inferior STEMI. JACC 8:161–169
12. Mitchell C, Rahko PS, Blauwet LA, Canaday B, Finstuen JA, Foster MC et al (2019) Guidelines for performing a comprehensive transthoracic echocardiographic examination in adults: recommendations from the American Society of Echocardiography. J Am Soc Echocardiogr 32:1–64
13. Schiller NB, Acquatella H, Ports TA, Drew D, Goerke J, Ringertz H et al (1979) Left ventricular volume from paired biplane two-dimensional echocardiography. Circulation 60(3):547–555
14. Lang RM, Badano LP, Mor-Avi V, Afilalo J, Armstrong A, Ernande L et al (2015) Recommendations for cardiac chamber quantification by echocardiography in adults: an update from the American Society of Echocardiography and the European Association of Cardiovascular Imaging. Eur Heart J Cardiovasc Imaging 16(3):233–271

15. de Simone G et al (1992) Left ventricular mass and body size in normotensive children and adults: assessment of allometric relations and impact of overweight. J Am Coll Cardiol 20(5):1251
16. Cerqueira MD, Weissman NJ, Dilsizian V, Jacobs AK, Kaul S, Laskey WK et al (2002) Standardized myocardial segmentation and nomenclature for tomographic imaging of the heart: a statement for healthcare professionals from the cardiac imaging committee of the council on clinical cardiology of the American Heart Association. Circulation 105:539–542
17. Holshue ML, DeBolt C, Lindquist S, Lofy KH, Wiesman J, Bruce H et al (2020) First case of 2019 novel coronavirus in the United States. N Engl J Med 382:929
18. Thygesen K, Alpert JS, Jaffe AS, Chaitman BR, Bax JJ, Morrow DA et al (2018) Fourth universal definition of myocardial infarction (2018). Eur Heart J 40(3):237–269
19. Blessberger H, Binder T (2010) Non-invasive imaging: Two dimensional speckle tracking echocardiography: basic principles. Heart 96:716–722
20. Mor-Avi V, Lang RM, Badano LP, Belohlavek M, Cardim NM, Derumeaux G et al (2011) Current and evolving echocardiographic techniques for the quantitative evaluation of cardiac mechanics: ASE/EAE consensus statement on methodology and indications endorsed by the Japanese Society of Echocardiography. J Am Soc Echocardiogr 24:277–313
21. Ancona R, Comenale Pinto S, Caso P, D'Andrea A, Di Salvo G, Arenga F et al (2014) Left atrium by echocardiography in clinical practice: from conventional methods to new echocardiographic techniques. Sci World J 2014:451042
22. Kalam K, Otahal P, Marwick TH (2014) Prognostic implications of global LV dysfunction: a systematic review and meta-analysis of global longitudinal strain and ejection fraction. Heart 100:1673–1680
23. Chan J, Hanekom L, Wong C, Leano R, Cho GY, Marwick TH (2006) Differentiation of subendocardial and transmural infarction using two-dimensional strain rate imaging to assess short-axis and long-axis myocardial function. J Am Coll Cardiol 48(2026–2033):6
24. Kang SJ, Lim HS, Choi BJ, Choi SY, Hwang GS, Yoon MH, Tahk SJ, Shin JH (2008) Longitudinal strain and torsion assessed by twodimensional speckle tracking correlate with the serum level of tissue inhibitor of matrix metalloproteinase-1, a marker of myocardial fibrosis, in patients with hypertension. J Am Soc Echocardiogr 21:907–911
25. Shah AM, Claggett B, Sweitzer NK, Shah SJ, Anand IS, Liu L, Pitt B, Pfeffer MA, Solomon SD (2015) Prognostic importance of impaired systolic function in heart failure with preserved ejection fraction and the impact of spironolactone. Circulation 132:402–414
26. Donal E, Lund LH, Oger E, Bosseau C, Reynaud A, Hage C, Drouet E, Daubert JC, Linde C, on behalf of the KaRen Investigators (2017) Importance of combined left atrial size and estimated pulmonary pressure for clinical outcome in patients presenting with heart failure with preserved ejection fraction. Eur Heart J Cardiovasc Imaging 18:629–635
27. Sanfilippo F, Corredor C, Fletcher N, Tritapepe L, Lorini FL, Arcadipane A, Vieillard-Baron A, Cecconi M (2018) Left ventricular systolic function evaluated by strain echocardiography and relationship with mortality in patients with severe sepsis or septic shock: a systematic review and meta-analysis. Crit Care 22:183
28. Zheng Z et al (2020) Risk factors of critical & mortal COVID-19 cases: a systematic literature review and meta-analysis. J Infect 81(2):e16–e25. https://doi.org/10.1016/j.jinf.2020.04.021
29. Tersalvi G et al (2020) Elevated troponin in patients with coronavirus disease 2019: possible mechanisms. J Cardiac Fail 26(6):470–475. https://doi.org/10.1016/j.cardfail.2020.04.009
30. Marques-Alves P, Espírito-Santo N, Baptista R et al (2018) Two-dimensional speckle-tracking global longitudinal strain in high-sensitivity troponin-negative low-risk patients with unstable angina: a "resting ischemia test"? Int J Cardiovasc Imaging 34(4):561–568
31. Inciardi RM, Lupi L, Zaccone G, Italia L et al (2020) Cardiac involvement in a patient with coronavirus disease 2019 (COVID-19). JAMA Cardiol 5:1
32. Clark JE, Marber MS (2013) Advancements in pressure-volume catheter technology—stress remodelling after infarction. Exp Physiol 98:614–621.24
33. Korff S, Katus HA, Giannitsis E (2006) Differential diagnosis ofelevated troponins. Heart 92:987–993
34. Li Y et al (2020) Prognostic value of right ventricular longitudinal strain in patients with COVID-19. JACC Cardiovasc Imaging. https://doi.org/10.1016/j.jcmg.2020.04.014
35. Bouhemad B, Nicolas-Robin A, Arbelot C, Arthaud M, Féger F, Rouby J-J (2009) Acute left ventricular dilatation and shock-induced myocardial dysfunction. Crit Care Med 37(2):441–447
36. Vieillard-Baron A, Caille V, Charron C, Belliard G, Page B, Jardin F (2008) Actual incidence of global left ventricular hypokinesia in adult septic shock. Crit Care Med 36(6):1701–1706
37. Peng Q-Y, Wang X-T, Zhang L-N (2020) Using echocardiography to guide the treatment of novel coronavirus pneumonia. BioMed Central 24:143
38. Furian T, Aguiar C, Prado K, Ribeiro RVP, Becker L, Martinelli N et al (2012) Ventricular dysfunction and dilation in severe sepsis and septic shock: relation to endothelial function and mortality. J Crit Care 27(3):319.e9–319.e15
39. Parker MM, McCarthy KE, Ognibene FP, Parrillo JE (1990) Right ventricular dysfunction and dilatation, similar to left ventricular changes, characterize the cardiac depression of septic shock in humans. Chest 97(1):126–131

Publisher's Note Springer Nature remains neutral with regard to jurisdictional claims in published maps and institutional affiliations.